Casimir manipulations: The orientation dependence of fluctuation-induced forces

T. Emig,[1,2] N. Graham,[3] R. L. Jaffe,[4] and M. Kardar[5]

[1] *Institut für Theoretische Physik, Universität zu Köln, Zülpicher Strasse 77, 50937 Köln, Germany*
[2] *Laboratoire de Physique Théorique et Modèles Statistiques, CNRS UMR 8626, Université Paris-Sud, 91405 Orsay, France*
[3] *Department of Physics, Middlebury College, Middlebury, VT 05753*
[4] *Center for Theoretical Physics, Laboratory for Nuclear Science, and Department of Physics, Massachusetts Institute of Technology, Cambridge, MA 02139, USA*
[5] *Department of Physics, Massachusetts Institute of Technology, Cambridge, MA 02139, USA*

(Dated: November 10, 2008)

The Casimir interaction between two objects, or between an object and a plane, depends on their relative orientations. We make these angular dependences explicit by considering prolate or oblate spheroids. The variation with orientation is calculated exactly at asymptotically large distances for the electromagnetic field, and at arbitrary separations for a scalar field. For a spheroid in front of a mirror, the leading term is orientation independent, and we find the optimal orientation from computations at higher order.

PACS numbers: 42.25.Fx, 03.70.+k, 12.20.-m. KITP report number: NSF-KITP-08-137

Casimir forces, predicted in 1948 [1] and probed in high precision experiments over the past decade [2, 3, 4, 5], are particularly important at micro-meter to nano-meter length scales. In constructing and manipulating devices at these length scales it is important to have an accurate understanding of the material, shape and orientation dependence of these forces. Since these dependencies often originate in the inherent many-body character of the force, they cannot be reliably obtained by commonly used approximations. In this Letter we investigate shape and orientation dependence of the Casimir force using a recently developed method [6] (see also [7]) that makes it possible to compute the Casimir interaction for arbitrary compact objects based on their scattering matrices.

A closely related work is the classic paper of Balian & Duplantier [8], which provides expressions for the large distance asymptotic force between perfectly conducting objects of arbitrary shape and orientation. Using our method, we generalize these results in a form suitable for extension to arbitrary dielectrics and distances. As tangible examples we then focus on ellipsoids, computing the orientation dependent force between two spheroids, and between a spheroid and a plane. The latter geometry is particularly interesting, as there in no orientation dependence *at leading order* for any object (metal or dielectric) in front of a mirror. We obtain the preferred orientation of a spheroid from a computation at higher order, in which T-matrices are evaluated in an expansion around a spherical shape. To numerically study a wider range of eccentricities and separations, we consider a scalar theory (in place of electromagnetism), for which efficient computations can be performed using a basis of spheroidal harmonics. For the case of Neumann boundary conditions, we find a transition in the preferred orientation as the spheroid approaches the plane.

We start from a general expression for the Casimir energy as an integral over imaginary wave number [6], of $\mathrm{Tr}\,\ln(1-\mathbb{N})$, which after expansion in powers of $\mathbb{N}$ reads

$$\mathcal{E}=-\frac{\hbar c}{2\pi}\int_0^\infty d\kappa\,\left[\mathrm{Tr}\,(\mathbb{N})+\frac{1}{2}\mathrm{Tr}\,\left(\mathbb{N}^2\right)+\cdots\right]. \qquad (1)$$

Here $\mathbb{N}=\mathbb{T}^1\mathbb{U}^{12}\mathbb{T}^2\mathbb{U}^{21}$, where $\mathbb{T}^1$ and $\mathbb{T}^2$ relate incoming and scattered electromagnetic (EM) fields, while the "translation matrix" $\mathbb{U}^{12}$ relates the incoming wave at one object to the outgoing wave at the other. Naturally, evaluating energies (and forces) from these formal expressions requires judicious choice of basis.

A natural basis for the field is (vector) spherical harmonic multipoles centered at each object, and labeled by (l,m,λ); the additional index $\lambda\in\{M,E\}$ distinguishes between transverse electric (TE) or magnetic (TM) modes. Each factor of $\mathbb{U}$ decays as $e^{-\kappa d}$, so we can obtain an asymptotic series, valid at large separations d. Since $\mathbb{T}^{\lambda\lambda}_{lm,l'm'}\propto\kappa^{l+l'+1}$, and $\mathbb{T}^{\lambda\sigma}_{lm,l'm'}\propto\kappa^{l+l'+2}$ for $\lambda\neq\sigma$, the expansion is dominated by the lowest order multipoles. Because electromagnetism does not admit monopole fluctuations, the leading asymptotic behavior comes from p-waves, $l=l'=1$. By examining the response of an object to a uniform electric (magnetic) field, it is straightforward to relate elements of the 3×3 matrix $\mathbb{T}^{EE}_{1m,1m'}$ ($\mathbb{T}^{MM}_{1m,1m'}$) to elements of the standard electric (magnetic) polarizability matrix α (β). In terms of the Cartesian components of the latter (with the $\hat{z}$ axis pointing from one object to the other), the first asymptotic contribution to the energy is

$$\begin{aligned}\mathcal{E}_1^{12} &= -\frac{\hbar c}{d^7}\frac{1}{8\pi}\Big\{13\left(\alpha^1_{xx}\alpha^2_{xx}+\alpha^1_{yy}\alpha^2_{yy}+2\alpha^1_{xy}\alpha^2_{xy}\right) \qquad (2)\\ &+ 20\,\alpha^1_{zz}\alpha^2_{zz}-30\left(\alpha^1_{xz}\alpha^2_{xz}+\alpha^1_{yz}\alpha^2_{yz}\right)+(\alpha\to\beta)\\ &- 7\left(\alpha^1_{xx}\beta^2_{yy}+\alpha^1_{yy}\beta^2_{xx}-2\alpha^1_{xy}\beta^2_{xy}\right)+(1\leftrightarrow2)\Big\},\end{aligned}$$

which generalizes the result of Balian and Duplantier [8] for perfectly conducting objects at nonzero temperatures. For the case of an ellipsoidal object with static electric permittivity ϵ and magnetic permeability μ, the polarizability tensors are diagonal in a basis oriented to its principal axes, with elements (for $i \in \{1,2,3\}$)

$$\alpha^0_{ii} = \frac{V}{4\pi}\frac{\epsilon-1}{1+(\epsilon-1)n_i}\,,\ \beta^0_{ii} = \frac{V}{4\pi}\frac{\mu-1}{1+(\mu-1)n_i}\,, \quad (3)$$

where $V = 4\pi r_1 r_2 r_3/3$ is the ellipsoid's volume and the so-called depolarizing factors are given by

$$n_i = \frac{r_1 r_2 r_3}{2}\int_0^\infty \frac{ds}{(s+r_i^2)\sqrt{(s+r_1^2)(s+r_2^2)(s+r_3^2)}}\,, \quad (4)$$

in terms of the semi-axis dimensions r_i. We can gain further insights into these results by focusing on the case of spheroids, for which $r_1 = r_2 = R$ and $r_3 = L/2$. Then the depolarizing factors can be expressed in terms of elementary functions,

$$n_1 = n_2 = \frac{1-n_3}{2},\ n_3 = \frac{1-e^2}{2e^3}\left(\log\frac{1+e}{1-e} - 2e\right), \quad (5)$$

where the eccentricity $e = \sqrt{1-\frac{4R^2}{L^2}}$ is real for a prolate spheroid ($L > 2R$) and imaginary for an oblate spheroid ($L < 2R$). The polarizability tensors for an arbitrary orientation are then obtained as $\alpha = \mathcal{R}^{-1}\alpha^0\mathcal{R}$, where $\mathcal{R}$ is the matrix that rotates the principal axis of the spheroid to the Cartesian basis, i.e. $\mathcal{R}(1,2,3) \to (x,y,z)$. The result provides the leading Casimir energy for spheroids of arbitrary size, orientation, and material. Note that for rarefied media with $\epsilon \simeq 1$, $\mu \simeq 1$ the polarizabilities are isotropic and proportional to the volume. Hence, to leading order in $\epsilon - 1$ the interaction is orientation independent at asymptotically large separations, as we would expect, since pairwise summation is valid for $\epsilon - 1 \ll 1$.

As a special case, we present the explicit formula for identical perfectly conducting prolate spheroids with the length $L \gg R$. To implement the perfect conductor limit, we take $\epsilon \to \infty$. In this limit, the full T-matrix is independent of μ. Because we are doing an expansion around zero frequency, however, we must set $\mu = 0$ to suppress the magnetic field that is still allowed at zero frequency. The orientation of each "needle" relative to the line joining them (the initial z-axis) is parameterized by the two angles (θ,ψ), as depicted in Fig. 1. Then

$$\begin{aligned}\mathcal{E}_1^{12}(\theta_1,\theta_2,\psi) \;=\; -\frac{\hbar c}{d^7}\Bigg\{&\frac{5L^6}{1152\pi\left(\ln\frac{L}{R}-1\right)^2}\times \quad (6)\\ &\Bigg[\cos^2\theta_1\cos^2\theta_2 + \frac{13}{20}\cos^2\psi\sin^2\theta_1\sin^2\theta_2\\ &-\frac{3}{8}\cos\psi\sin 2\theta_1\sin 2\theta_2\Bigg] + \mathcal{O}\left(\frac{L^4R^2}{\ln\frac{L}{R}}\right)\Bigg\},\end{aligned}$$

where $\psi \equiv \psi_1 - \psi_2$.

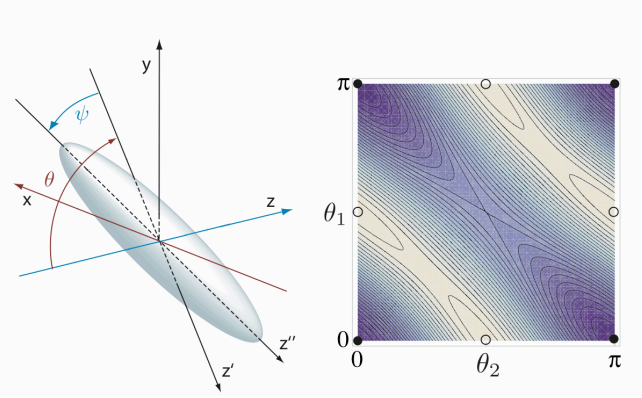

FIG. 1: Orientation of a prolate (cigar-shaped) spheroid: The symmetry axis (initially the z-axis) is rotated by θ about the x-axis and then by ψ about the z-axis. For two such spheroids, the energy at large distances is give by Eq. (6). The latter is depicted at fixed distance d, and for $\psi_1 = \psi_2$, by a contour plot as function of the angles θ_1, θ_2 for the x-axis rotations . Minima (maxima) are marked by filled (open) dots.

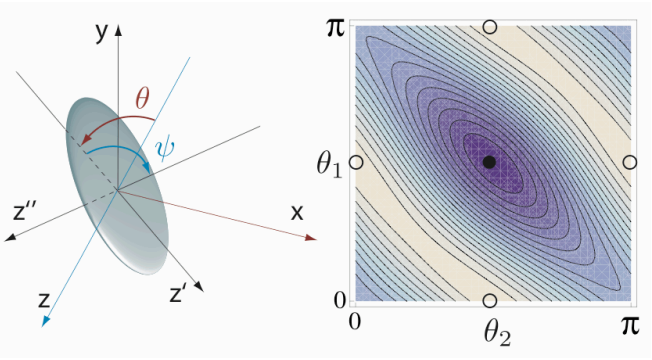

FIG. 2: As in Fig. 1 for oblate (pancake-shaped) spheroids, with a contour plot of energy at large separations.

We note the following features of this result:

- The energy is minimized for $\theta_1 = \theta_2 = 0$, i.e., for two needles aligned parallel to their separation vector, as we expect since this case is dominated by the fluctuations of electric dipoles along the symmetry axis.
- At almost all orientations the energy scales as L^6, and vanishes logarithmically slowly as $R \to 0$.
- The dependence vanishes when one needle is orthogonal to $\hat{z}$ (i.e. $\theta_1 = \pi/2$), while the other is either parallel to $\hat{z}$ ($\theta_2 = 0$) or has an arbitrary θ_2 but differs by an angle $\pi/2$ in its rotation about the z-axis (i.e. $\psi_1 - \psi_2 = \pi/2$). In these cases the energy comes from the next order term in Eq. (6), and takes the form

$$\mathcal{E}_1^{12}\left(\frac{\pi}{2},\theta_2,\frac{\pi}{2}\right) = -\frac{\hbar c}{1152\pi\, d^7}\frac{L^4R^2}{\ln\frac{L}{R}-1}\left(73+7\cos 2\theta_2\right). \quad (7)$$

- From Eq. (7) we see that the least favorable configuration ($\theta_2 = \pi/2$) corresponds to two needles orthogonal to each other and to the line joining them.

For perfectly conducting oblate spheroids with $R \gg$

$L/2$, the orientation of each "pancake" is again described by a pair of angles (θ, ψ), as depicted in Fig. 2. A contour plot of the leading angular dependence is also presented in the figure; its explicit formula will not be reproduced here, but we note the following features:

• The leading dependence is proportional to R^6, and does not disappear for any choice of orientations. Furthermore, this dependence remains even as the thickness of the pancake is taken to zero ($L \to 0$). This is very different from the case of the needles, where the interaction energy vanishes with thickness as $\ln^{-1}(L/R)$. We attribute this effect to dimensionality: The limiting linear needle is only marginally visible to the EM field, while the limiting two dimensional plane remains as an opaque obstacle. The lack of L dependence is due to the assumed perfectly metallic screening. If the dielectric function remains finite in the static limit, a conventional scaling with volumes of the objects is expected.

• The configuration of minimal energy corresponds to two pancakes lying on the same plane ($\theta_1 = \theta_2 = \pi/2$, $\psi = 0$) and has energy $-\hbar c\,(173/18\pi^3)R^6/d^7$. This is due to the electric dipole fluctuations in the planes.

• When the two pancakes are stacked on top of each other, the energy is increased to $-\hbar c\,(62/9\pi^3)R^6/d^7$.

• The least favorable configuration is when the pancakes lie in perpendicular planes, i.e., $\theta_1 = \pi/2$, $\theta_2 = 0$, with an energy $-\hbar c\,(11/3\pi^3)R^6/d^7$.

For an object interacting with a perfectly reflecting mirror, we can use its image to construct $\mathbb{N} = -\tilde{\mathbb{T}}^1\tilde{\mathbb{U}}^{R,11}$, where R stands for the reflected object [10]. Alternatively, we can express the scattering matrix for the mirror in a basis of plane waves, and use a translation matrix to convert between this basis and the basis for scattering of the compact object. At leading order we have

$$\mathcal{E}_1^{1m} = -\frac{\hbar c}{d^4}\frac{1}{8\pi}\mathrm{Tr}(\alpha - \beta) + \mathcal{O}(d^{-5})\,, \tag{8}$$

which is clearly independent of orientation. A similar expression for a mirror and an atom is present in the classic work of Casimir and Polder [1], and implicit in Ref. [8] for perfect conductors. (The orientation independence of energy is special to zero temperature; at nonzero temperatures the general expression in Ref. [8] does contain angular dependence.) Orientation dependence in this system thus comes from higher multipoles. The next order also vanishes, so the leading term is the $l = 3$ contribution to the term linear in $\mathbb{N}$ in Eq. (1), in which case the scattering matrix is not known analytically.

Instead, we obtained the preferred orientation by considering a distorted sphere in which the radius R is deformed to $R + \delta f(\vartheta, \varphi)$. The function f can be expanded into spherical harmonics $Y_{lm}(\vartheta, \varphi)$, and spheroidal symmetry can be mimicked by choosing $f = Y_{20}(\vartheta, \varphi)$. By performing a perturbative expansion of spherical T-matrices in δ, the leading orientation dependent part of the energy is obtained as

$$\mathcal{E}_f = -\hbar c\frac{1607}{640\sqrt{5}\pi^{3/2}}\frac{\delta R^4}{d^6}\cos(2\theta)\,. \tag{9}$$

A prolate spheroid ($\delta > 0$) thus minimizes its energy by pointing towards the mirror, while an oblate spheroid ($\delta < 0$) prefers to lie in a plane perpendicular to the mirror. (We assume that the perturbative results are not changed for large distortions.) These configurations are also preferred at small distances d, since (at fixed distance to the center) the object reorients to minimize the closest separation.

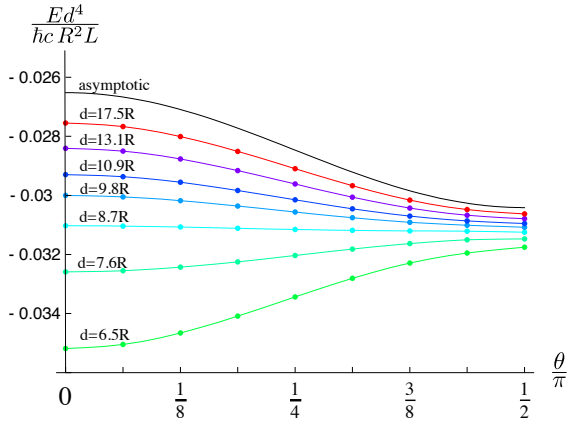

FIG. 3: The orientation dependence of the Casimir energy for a prolate Neumann spheroid with $L/R = 4.8$ opposite a Neumann plane, as a function of the angle θ between the normal to the plane and the spheroid axis, for various values of d, the distance from the spheroid center to the plane. The asymptotic result of Eq. (12) is depicted by the top line. For $d \lesssim 8.5R$, the spheroid prefers to point toward the plane, while at larger distances it spontaneously breaks the rotational symmetry and aligns parallel to the plane. The larger the value of $\xi_0 = 1/e$, the larger the distance at which this transition occurs.

Interestingly, the above conclusion is not generally true, and as discussed below, we find that there can be a transition in preferred orientation as a function of d in the simpler case of a scalar field. Then we can obtain the T-matrices and translation matrices as straightforward generalizations of the spherical case, in which spherical harmonics and Bessel functions are replaced by spheroidal harmonics and spheroidal radial functions. Prolate spheroidal coordinates [11] are defined by taking ϕ as the usual azimuthal angle and

$$\sqrt{x^2 + y^2} \;=\; a\sqrt{(\xi^2 - 1)(1 - \eta^2)}, \quad z = a\eta\xi\,, \tag{10}$$

where the interfocal separation is $2a$. The surface of the spheroid is defined by a constant spheroidal radius $\xi = \xi_0 = 1/e$, with $L = 2\xi_0 a$ and $R = a\sqrt{\xi_0^2 - 1}$. Oblate coordinates are obtained by analytic continuation of the

radial coordinate with $\xi \to -i\xi$ and $k \to ik$. We use the conventions of Ref. [12] in which the spheroidal functions are normalized identically to their spherical analogs.

The T-matrix is diagonal, with elements which in terms of radial spheroidal functions of the first and third kinds are $T^S_{lm}(i\kappa) = -\frac{R_l^{m(1)\prime}(i\kappa a;\xi_0)}{R_l^{m(3)\prime}(i\kappa a;\xi_0)}$, where the prime indicates derivative with respect to the second argument. The translation matrix converts between the spheroidal basis, indexed by l and m, and the plane wave basis, indexed by the momentum parallel to the plane $\boldsymbol{q}_\perp$. The calculation is performed on the imaginary axis; with $q_\perp$ real, and $q_\parallel \equiv i\sqrt{\kappa^2 + q_\perp^2}$, which is pure imaginary. The translation matrix element $U^{\boldsymbol{q}_\perp}_{lm}(i\kappa)$ at separation L is $U^{q_\perp,\phi_q}_{lm} = i^l(-1)^m \frac{e^{iq_\parallel L}}{q_\parallel} \mathcal{Y}_l^{-m}(i\kappa a, \eta, \phi)$, where $\mathcal{Y}_l^m$ is a spheroidal harmonic and $\eta = \frac{q_\parallel \cos\theta - q_\perp \cos\phi_q \sin\theta}{i\kappa}$. Here, θ is the angle between the spheroid axis and the normal to the plane and $\tan\phi = \frac{q_\perp \sin\phi_q}{q_\parallel \sin\theta + q_\perp \cos\theta \cos\phi_q}$, where ϕ_q is the polar angle of $\boldsymbol{q}_\perp$ around the perpendicular to the plane. To implement the matrix multiplication needed to compute $\mathbb{N}$, we integrate over $\boldsymbol{q}_\perp$. Normalizing the integration measure introduces a factor of $2q_\parallel/(i\kappa)$.

The numerical results can be compared to the large distance expansion for an object with Neumann boundary conditions that is placed opposite to a plane (the latter with Dirichlet or Neumann boundary conditions). The general form of the energy in this case is

$$\mathcal{E} = \pm\frac{\hbar c}{d^4}\left[\frac{1}{64\pi^2}V - \frac{1}{16\pi}(\beta_{xx} + \beta_{yy} + 3\beta_{zz})\right], \quad (11)$$

for a Dirichlet/Neumann $(+/-)$ plane, where V is the volume, and β is like the static magnetic polarizability tensor in Eq. (3) for $\mu = 0$. For a spheroid this results in

$$\mathcal{E} = \pm\frac{\hbar c}{d^4}\frac{R^2 L}{96\pi}\frac{9 - 4n_3 - n_3^2 + (3n_3 - 1)\cos 2\theta}{1 - n_3^2}, \quad (12)$$

where n_3 is given by Eq. (5). In contrast to the EM energy of Eq. (8), the leading term of Eq. (12) is orientation dependent. For a prolate spheroid with $R \ll L$ we have

$$\mathcal{E} = \pm\frac{\hbar c}{d^4}\frac{R^2 L}{96\pi}\left[9 - \cos(2\theta) + \mathcal{O}((R/L)^2)\right], \quad (13)$$

and for an oblate spheroid with $R \gg L$, we have

$$\mathcal{E} = \pm\frac{\hbar c}{d^4}\frac{R^3}{24\pi^2}\left[2 + \cos(2\theta) + \mathcal{O}((L/R))\right]. \quad (14)$$

To leading order in R/L and at fixed separation d, the energy for a Neumann plate is minimized at $\theta = \pi/2$ for a prolate spheroid and at $\theta = 0$ for an oblate spheroid. This means that both a needle and a pancake prefer to be parallel to the plate; in the former case because of β_{xx} and β_{yy} and in the latter case because of β_{zz}. For a Dirichlet plate, the energy is minimal if the needle or the pancake are perpendicular to the plate as would have been predicted by pairwise summation.

In Fig. 3 we present a sample of the full numerical calculation, using an optimized version [13] of the spheroidal harmonic package of Falloon [14]. We truncate the infinite sum at $l = 2$, though we have verified for individual cases that summing through $l = 4$ does not significantly change these results. At close separations, the prolate spheroid prefers to point toward the plane, as we expect from the proximity force approximation. At large separations, we have shown that the configuration parallel to the plane has the lowest energy. We thus observe a spontaneous breaking of the symmetry around the perpendicular to the plane; the separation at which this transition occurs varies with the spheroid's eccentricity.

These examples provide a glimpse into the myriad effects of shape and orientation on the Casimir effect. One can imagine that with better precision of experiment and theory such forces can be employed to manipulate small objects at the micro- and nano-meter scales.

We acknowledge discussions with S. J. Rahi. This research was supported by the DFG through grant EM70/3 (TE), and NSF grants DMR-08-03315 (MK), PHY-0555338 (NG), a Cottrell College Science Award from Research Corporation (NG), and the U. S. Department of Energy under cooperative research agreement #DF-FC02-94ER40818 (RLJ). Part of this work was carried out at the Kavli Institute for Theoretical Physics, with support from NSF Grant No. PHY05-51164.

[1] H. B. G. Casimir and D. Polder, Phys. Rev. **73**, 360 (1948); H. B. G. Casimir, Proc. K. Ned. Akad. Wet. **51**, 793 (1948).
[2] S. K. Lamoreaux, Phys. Rev. Lett. **78**, 5 (1997).
[3] U. Mohideen and A. Roy, Phys. Rev. Lett. **81**, 4549 (1998).
[4] G. Bressi, G. Carugno, R. Onofrio, and G. Ruoso, Phys. Rev. Lett. **88**, 041804 (2002).
[5] H. B. Chan, V. A. Aksyuk, R. N. Kleiman, D. J. Bishop, and F. Capasso, Science **291**, 1941 (2001).
[6] T. Emig, N. Graham, R. L. Jaffe, and M. Kardar, Phys. Rev. Lett. **99**, 170403 (2007); Phys. Rev. D **77**, 025005 (2008).
[7] O. Kenneth and I. Klich, Phys. Rev. B **78**, 014103 (2008).
[8] R. Balian and B. Duplantier, Ann. Phys. **104**, 300 (1977); **112**, 165 (1978).
[9] F. M. Schulz, K. Stamnes, and J. J. Stamnes, Appl. Optics **37**, 7875 (1998).
[10] T. Emig, J. Stat. Mech. P04007 (2008).
[11] C. Flammer, *Spheroidal Wave Functions* (Stanford University Press, Stanford, 1957).
[12] N. Graham and K. D. Olum, Phys. Rev. D **72**, 025013 (2005).
[13] See `http://community.middlebury.edu/~ngraham`.
[14] P. E. Falloon, P. C. Abbott, and J. B. Wang, J. Phys. **A36** (2003) 5477.